Analysis of Cell Association in mmWave Networks based on Euclidean and Angular Distances

Charalampos (Harris) K. Armeniakos*, Athanasios G. Kanatas* and Harpreet S. Dhillon†
*Department of Digital Systems, University of Piraeus, Piraeus, Greece
†Bradley Department of Electrical and Computer Engineering, Virginia Tech, Blacksburg, VA, 24061, USA
Email: {harmen,kanatas}@unipi.gr, hdhillon@vt.edu

***Abstract*—In millimeter wave (mmWave) networks, the communication link performance is heavily dependent on the directional characteristics of the transceiver beams. Under practical beam management considerations, the transmitter and receiver beams may not be perfectly aligned. We consider such a situation in the downlink of a mmWave cellular network. In this case, the received powers from the base stations (BSs) at the user equipment (UE) of interest will depend upon both the Euclidean and the angular distances (of the BSs to that UE). We develop a novel stochastic geometry framework to study maximum power-based association in this setting. To the best of our knowledge, this is the first work that rigorously explores the role of angular distances in the association policy and analysis of cellular networks. We derive exact expressions for the distributions of signal-to-interference-plus-noise ratio (SINR) and the link rate, as well as the average achievable rate. Among others, our analysis reveals that as the receiver beam becomes more directional (i) the instantaneous achievable rate improves at the expense of a significantly higher variance, and (ii) both the desired received power and the interference power decrease because of the reduced misalignment error and the reduction of the number of interfering BSs falling within in the 3 dB beamwidth of the receiver antenna pattern, respectively, and (iii) the probability of achieving a higher target rate than the average increases.**

***Index Terms*—6G, 5G NR, beam management, coverage probability, millimeter-wave communication, stochastic geometry.**

I. Introduction

It is well accepted that higher frequency bands, especially at the millimeter wave (mmWave) frequencies and in the near future at the sub-terahertz frequencies, are essential for supporting emerging data-hungry applications, such as extended reality and 3D gaming [1]. In the context of commercial fifth generation (5G) new radio (NR) cellular standard, mmWave communication has attracted considerable attention from both academia and industry over the past decade [2], [3]. To overcome the challenging propagation characteristics which come with the extremely high data rates, mmWave networks are envisioned to be densely deployed to achieve acceptable coverage [4]. However, increasing the density of BSs leads to severe interference problems. The resulting interference may cause a significant number of transmission failures, especially for dense mmWave networks. Therefore, antenna arrays with highly directional and steerable antenna beams are necessary to achieve high power gain and improved coverage.

Owing to the large number of beams typically considered for mmWave links, a series of beam management procedures are needed to ensure efficient handling and network operation. The selection of the best receiving beam is performed in mmWave networks by measuring the average received signal power in each beam through exhaustive scanning from a set of candidate serving BSs. In this setting, the maximum power-based association decisions are governed by the distance dependent path loss and the transmitting and receiving antenna gain patterns. By assuming simplistic antenna patterns, such as the flat-top pattern [5], [6], or by making other idealistic assumptions, such as perfect channel estimation and beam training, prior works often assume perfect alignment in the transmitting beam from the BS and the receiving beam at the UE [7], [8]. In such cases, the cell association decision ends up being a function of just the Euclidean distances between the receiver and candidate serving BSs, which is a significant simplification of reality.

In realistic mmWave networks, beam misalignment is inevitable, and the directions of the maximum gains at the BS and UE are not fully aligned [9]. For realistic antenna patterns, the misalignment error now naturally becomes a function of the angular distance between the candidate serving BSs and the UE. In this case, both the Euclidean and the angular distance of the candidate serving BSs should be jointly considered in the measurement of the received power during the association phase. Recently, in [10], the notion of angular distances was addressed and their relevance in the performance analysis of mmWave networks was highlighted. Subsequently, in [11], the angular distances were considered in the calculation of the interference power by exploiting realistic antenna patterns. However, perfect alignment between the direction of the UE's and the serving BS's maximum gain was assumed. *To the best of the authors' knowledge, this is the first work that rigorously explores the role of angular distances in the association policy and performance analysis of cellular networks*.

In this paper, a tractable stochastic geometry framework is proposed to account for realistic 5G NR beam management-based procedures by jointly considering both the Euclidean and the angular distances of the candidate serving BSs in the UE's association policy. To this end, the UE, which is equipped with a realistic 3GPP-based antenna pattern, exploits directional beamforming capabilities under imperfect alignment to communicate with the serving BS. Subsequently, performance analysis in terms of the distributions of the SINR and the like rate, as well as the average achievable rate is conducted under the proposed novel association scheme and exact-form

analytical expressions are derived. As key intermediate results, the probability density function (pdf) of the maximum received power and the Laplace transform of the aggregate interference power distribution are also obtained in exact form.

II. System Model And Proposed Framework

A. Network Model

Consider a mmWave downlink cellular network, where the locations of the BSs are modeled as a homogeneous Poisson point processes (HPPP) $\Phi_{bs} \subset \mathbb{R}^2$ with intensity λ_{bs}. Let (r_x, ϕ_x) denote the polar coordinates of the location of a BS placed at $x \in \Phi_{bs}$. The locations of UEs are independently distributed according to some stationary point process Φ_{ue}. Also, all BSs are assumed to transmit at the same power p. Let (r_s, ϕ_s) denote the polar coordinates of the location of the serving BS $x_0 \in \Phi_{bs}$ at a given time. Without loss of generality, the receiving UE is assumed to be located at the origin $\mathbf{o} = (0, 0)$ at that time. After averaging the performance of this UE over Φ_{bs}, the receiving UE becomes the typical receiver, which we will simply term the *receiver*.

Considering the pertinent properties of mmWave communications, a BS located at $x \in \Phi_{bs}$ is assumed to exploit proper directional beamforming techniques to communicate with the receiver assuming perfect channel state information (CSI). Therefore, the maximum gain of the BSs' antennas can be assumed to be always directed towards the receiver. The receiver is assumed to be equipped with an antenna array able to produce 2^m receiving beams. The maximum gain directions of these beams, i.e., the centers of the corresponding 3 dB beamwidths, are given by $\phi_m = \frac{2\pi}{2^m}$ with $m \in \mathbb{N}$. Please note that the maximums of the BS and UE beams will not necessarily be aligned because of the discretization on the UE side, which is the reason angular distances appear in the analysis. In this work, a realistic 3GPP-based antenna pattern recommended for 5G mmWave communications [12] is adopted for the receiver and therefore, the actual antenna gain within the 3dB beamwidth range is not constant. When directed towards ϕ_0^r, this antenna has a radiation power pattern (in dB) given by

$$G_{3gpp}(\phi - \phi_0^r) = G_{max} - \min\left\{12\left(\frac{\phi - \phi_0^r}{\phi_{3dB}}\right)^2, SLA\right\}, \quad (1)$$

where ϕ_{3dB} is the 3dB beamwidth of the receiver's antenna and $SLA = 30$dB is the front-to-back ratio. The multiplicative antenna gain factor is denoted by $g_{3gpp}(\phi - \phi_0^r)$. The direction of maximum gain ϕ_0^r is modeled as a discrete random variable with probability mass function (pmf) given by

$$\phi_0^r = \begin{cases} \phi_0^1 = \frac{\pi}{2^m}, & \text{w.p. } p_\phi = \frac{1}{2^m} \\ \phi_0^2 = \frac{\pi}{2^m} + \frac{\pi}{2^{m-1}}, & \text{w.p. } p_\phi = \frac{1}{2^m} \\ \vdots & \\ \phi_0^{2^m} = \frac{\pi}{2^m} + \underbrace{\frac{\pi}{2^{m-1}} + \ldots + \frac{\pi}{2^{m-1}}}_{(2^m-1)\text{ terms}}, & \text{w.p. } p_\phi = \frac{1}{2^m} \end{cases} \quad (2)$$

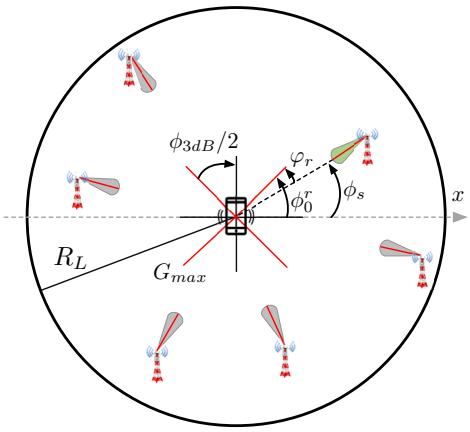

Fig. 1: Illustration of the system model.

A representative example of ϕ_0^r is shown in Fig. 1, with $2^m = 4$ beams enabled at the UE. Unfortunately, performance analysis using the array pattern of (1) may lead to extremely intractable analysis [7]. For this reason, the array pattern is approximated by the two-branch expression given by [13],

$$g(\phi - \phi_0^r) = \begin{cases} g_{max} 10^{-\frac{3}{10}\left(\frac{2(\phi-\phi_0^r)}{\phi_{3dB}}\right)^2}, & |\phi - \phi_0^r| \le \phi_A \\ g_s, & \phi_A \le |\phi - \phi_0^r| \le \pi \end{cases} \quad (3)$$

where g_{max} and g_s are the multiplicative gain factors of G_{max}, and $G_s = G_{max} - SLA$, correspondingly, whereas $\phi_A = (\phi_{3dB}/2)\sqrt{(10/3)\log_{10}(g_{max}/g_s)}$.

As seen from the receiver location, a BS can be either LOS or non-LOS (NLOS). Since mmWave signals are susceptible to blockages [14], proper modeling is essential to capture the effect of blockages on network performance. Accordingly, a LOS ball model is adopted since it provides a better fit with real-world blockage scenarios [15]. Given a BS located at $x \in \Phi_{bs}$, the propagation between the BS and the receiver is LOS if $\|x\| < R_L$, where R_L is the maximum distance for LOS propagation and $\|\cdot\|$ denotes the Euclidean norm. In this work, the performance analysis for the receiver is restricted to $\mathbf{b}(\mathbf{o}, R_L)$, where $\mathbf{b}(\mathbf{o}, R_L)$ denotes a LOS ball of radius R_L centered at the origin $\mathbf{o}$.[1] Accordingly, the analysis is restricted to a finite HPPP $\Psi_{bs} = x \in \Phi_{bs} \cap \mathbf{b}(\mathbf{o}, R_L)$.

Let α_L denote the path loss exponent for the LOS propagation links. Similar to [5], typical values of α_L are $\alpha_L \in [1.8, 2.5]$. Then, following the standard power-law path-loss model for the path between the receiver and a BS located at $x \in \Psi_{bs}$, the path loss function is denoted by $l(\|x\|) = K\|x\|^{-\alpha_L}$, where $K = \left(\frac{c}{4\pi f_c}\right)^2$ with c being the speed of light and f_c the carrier frequency.

The wireless channel between a BS located at $x \in \Psi_{bs}$ and the receiver undergo Nakagami-m_u fading, which allows us to

[1]The received signal power from the BSs outside the LOS ball is considered negligible due to the severe path loss imposed by the blockages [4], [16]. Moreover, the authors in [17] have shown that NLOS links have negligible effect on the system coverage performance in dense mmWave networks.

represent a wide range of fading environments. The parameter m_u is restricted to integer values for analytical tractability. The channel fading gain h_u is the fading power for the channel in the LOS condition. The shape and scale parameters of h_u are m_u and $1/m_u$, respectively, i.e., $h_u \sim$ Gamma $\left(m_u, \frac{1}{m_u}\right)$. Here, $u \in \{s, x\}$, where s denotes the link between the receiver and the serving BS, and x stands for the link between the receiver and the interfering BSs at $x \in \Psi_{bs} \setminus \{x_0\}$. The pdf of h_u is given by

$$f_{h_u}(w) = \frac{m_u^{m_u} w^{m_u - 1}}{\Gamma(m_u)} \exp\left(-m_u w\right). \tag{4}$$

Note that $\mathbb{E}[h_u] = 1$, where $\mathbb{E}[\cdot]$ denotes expectation.

B. User Association and Beam Selection Policy

The association policy used in real networks is often based on the maximum received power. The UE is agnostic to the conditions that provide the maximum power to the receiver. One of the main contributions of this paper is the adoption of an association policy, namely *5G NR maximum power association policy*, that accurately captures realistic conditions. Accordingly, in this scheme the UE is associated with the BS providing the largest average received power by jointly considering both the Euclidean and the angular distances of the BSs when the best receiving beam is selected for reception. According to the beam management procedure in 5G NR, this task is the so-called *beam selection procedure*. In particular, all BSs periodically transmit the beamformed reference signals that may cover the entire set of available directions according to the receivers' needs. The mmWave-based measurements for initial access are based on the synchronization signal blocks (SSBs). The receiver in the proposed framework monitors the reference signals and forms a list of candidate serving BSs, defined as the ones with the largest SNR, if above a predefined threshold, for each beam. Subsequently, *the serving BS*, defined as the BS providing the largest SNR among *all* candidate serving BSs, is chosen for transmission. The corresponding receiver's beam in which the serving BS was identified, is selected as the *receiving beam*.

The BSs are assumed to have perfect CSI knowledge of the uplink and thus, a perfect alignment of the BSs' beam maximum gain direction with the line toward the receiver is achievable. On the other hand, the direction of the maximum gain of the receiver's antenna is not fully aligned with the direction of maximum gain of each BS transmitting beam. Let φ_i^x denote the angular distance between the direction of the line connecting the receiver and a BS $x \in \Psi_{bs}$ and the direction, ϕ_0^i, of maximum directivity of a receiver's beam i. Therefore, for a BS $x \in \Psi_{bs}$, ϕ_x denotes its polar coordinate, and φ_i^x is given by $\varphi_i^x = |\phi_0^i - \phi_x|$. By further considering the Euclidean distances of the BSs from the origin, r_x, the location of the serving BS and the receiving beam are chosen by the receiver as

$$(x_0, i) = \underset{\substack{x \in \Psi_{bs} \\ i = 1:2^m}}{\operatorname{argmax}} \left\{ g(\varphi_i^x) r_x^{-\alpha_L} \right\}. \tag{5}$$

Having selected x_0 and i, the angle φ_i^x is denoted as φ_r in Fig. 1. In this case, φ_r can be modeled as a uniform random variable, i.e., $\varphi_r \sim U[0, \frac{\phi_{3dB}}{2}]$. Clearly, the serving BS may not necessarily be the nearest one to the receiver. Instead, it may lie close to the direction of the maximum directivity gain of a receiver's beam and thus provide maximum received power. Eq. (5) indicates that the receiver performs scanning for each beam to identify the serving BS by jointly considering both the angular distance of the BSs, from the direction of each beam's maxima, and the Euclidean distance of the BSs, respectively to maximize the received power.

C. Performance Metrics

Under the aforementioned 5G NR maximum power policy, the received SINR is given by

$$\text{SINR} = \frac{p\, h_s\, g_{max}\, g(\varphi_r)\, l(\|x_0\|)}{I + \sigma^2}, \tag{6}$$

where I refers to the aggregate interference power and is given by $I = \sum_{x \in \Psi_{bs}^!} p\, h_x\, g_{max}\, g_{3gpp}(\varphi_I)\, l(\|x\|)$, $\Psi_{bs}^! = \left\{\Psi_{bs} \setminus \{x_0\}\right\}$, φ_I is defined as $\varphi_I = |\phi_0^r - \phi_x|$ and σ^2 is the additive white Gaussian noise power. Please note that, ϕ_0^r also determines the direction of the reference line.

The network performance will be characterized in terms of the SINR-based coverage probability, which is defined as the probability that the SINR at the receiver in $\mathbf{b}(\mathbf{o}, R_L)$ exceeds a predefined threshold γ_{th}, i.e., $\mathcal{P}_c(\gamma_{th}) \triangleq \mathbb{P}(\text{SINR} \geqslant \gamma_{th})$. We will also consider the following achievable rate-related metrics: i) the rate coverage which can be mathematically expressed as $\mathcal{R}_c(R_{th}) = \mathbb{P}[B_w \log_2(1 + \text{SINR}) \geq R_{th}]$, where R_{th} is the target rate and B_w is the bandwidth available to the link of interest, and ii) the average achievable rate of the UE, which can be mathematically expressed as $\mathcal{R} \triangleq \mathbb{E}[B_w \log_2(1 + \text{SINR})])$.

III. Performance Analysis

In this section we present the comprehensive analysis in terms of the performance metrics defined above. The pdf of the maximum received power must first be derived. Let S_x^i denote the received power from a BS located at $x \in \Psi_{bs}$ measured w.r.t to the i-th beam. Then, S_x^i is given by

$$S_x^i = g(|\phi_0^i - \phi_x|)\|x\|^{-\alpha_L} = g(|\phi_0^i - \phi_x|) r_x^{-\alpha_L}, \tag{7}$$

and the maximum received power S is obtained as

$$S = \max_{\substack{x \in \Psi_{bs} \\ i = 1:2^m}} \{S_x^i\} \overset{(a)}{=} \max_{x \in \Psi_{bs}} \{\underbrace{g(\varphi_r) r_x^{-\alpha_L}}_{S_x}\} \overset{(b)}{=} g(\varphi_r) r_s^{-\alpha_L}, \tag{8}$$

where (a) follows from the independence between ϕ_x and r_x of the BSs and maximization over $\{g(|\phi_0^i - \phi_x|)\}_{\substack{i=1:2^m \\ x \in \Psi_{bs}}}$ and (b) follows from maximization over $\{r_x^{-\alpha_L}\}_{x \in \Psi_{bs}}$ with $r_s = \|x_0\|$. Due to exhaustive scanning of the receiver in the whole $\mathbf{b}(\mathbf{o}, R_L)$, the serving BS may lie anywhere in $\mathbf{b}(\mathbf{o}, R_L)$. Therefore, the distances $\{r_x\}$ are independent and identically distributed (i.i.d.) in $\mathbf{b}(\mathbf{o}, R_L)$ with pdf $f_{r_x}(r)$ of each element given by $f_{r_x}(r) = \frac{2r}{R_L^2}$, $r \in [0, R_L]$. The pdf of S is now derived, as a key intermediate result in the analysis.

Lemma 1. *The pdf of the maximum received power S is given by*

$$f_S(s_0) = \lambda_{bs}\pi R_L^2 \, f_{S_x}(s_0)\, e^{\lambda_{bs}\pi R_L^2 \left(\int_{w_{min}}^{s_0} f_{S_x}(w)\mathrm{d}w - 1\right)}, \quad (9)$$

$s_0 \in [w_{min}, \infty)$ *and* $f_{S_x}(w)$ *is given by*

$$f_{S_x}(w) = \int_{g_{3dB}}^{\psi(w)} \frac{1}{x} f_{g(\varphi_r)}(x) f_{r_x^{-\alpha_L}}\left(\frac{w}{x}\right)\mathrm{d}x, \quad (10)$$

$w \in [w_{min}, \infty)$ *where* $f_{r_x^{-\alpha_L}}(x) = \frac{2(\frac{1}{x})^{\frac{\alpha_L+2}{\alpha_L}}}{\alpha_L R_L^2}$, $f_{g(\varphi_r)}(g) = \frac{1}{ln(10)x}\frac{10}{12\sqrt{\frac{G_{max}-10log(x)}{12}}}$, $g_{3dB} = 10^{\frac{G_{max}-3}{10}}$, $w_{min} = g_{3dB}R_L^{-\alpha_L}$ *and* $\psi(w) = \min\left\{\frac{w}{R_L^{-\alpha_L}}, g_{max}\right\}$.

Proof. See Appendix A. ■

Lemma 2. *Conditioned on the maximum received power $S = S_{th}$ from the serving BS w.r.t. a given receiving beam, the conditional Laplace transform $\mathcal{L}_I(s|S_{th}, \phi_0^r)$ of the aggregate interference power distribution is given by (11), shown at the bottom of the page, where*

$$\mathbf{\Omega} = \{(r_x, \phi_x) \in \Psi_{bs}^! | r_x^{min} \le r_x \le R_L,\, 0 \le \phi_x \le 2\pi\}, \quad (12)$$

and $r_x^{min} = \min\left\{\left(\frac{g_{3gpp}(|\phi_0^r - \phi_x|)}{S_{th}}\right)^{\frac{1}{\alpha_L}}, R_L\right\}$.

Proof. The proof is delegated to the expanded journal version of this paper (preprint available on arXiv [18]) because of the lack of space. ■

Theorem 1. *The coverage probability of a receiver in a mmWave network inside $\mathbf{b}(\mathbf{o}, R_L)$ under the 5G NR maximum power association policy is given by*

$$\mathcal{P}_c(\gamma) = \sum_{i=1}^{2^m}\sum_{k=0}^{m_s-1}\int_{w_{min}}^{\infty} \frac{(-s)^k}{k!}\left[\frac{\partial^k \mathcal{L}_{I_{tot}}(s|S_{th}, \phi_0^i)}{\partial s^k}\right]_s \times f_S(S_{th}) p_\phi \mathrm{d}S_{th}, \quad (13)$$

where $s = \frac{m_s \gamma}{p\, g_{max}\, K\, S_{th}}$ *and* $\mathcal{L}_{I_{tot}}(s|S_{th}, \phi_0^i) = \exp(-\sigma^2 s)\mathcal{L}_I(s|S_{th}, \phi_0^i)$.

Proof. The conditional coverage probability is first given by

$$\begin{aligned}
\mathcal{P}_c(\gamma) &= \mathbb{P}\Big[\frac{p\, h_s\, g_{max}\, g(\varphi_r)\, l(\|x_0\|)}{I + \sigma^2} > \gamma \Big| r_s, \phi_s, \phi_0^r\Big] \\
&= \mathbb{P}\Big[\frac{p\, h_s\, g_{max}\, K\, S_{th}}{I + \sigma^2} > \gamma \Big| S_{th}, \phi_0^r\Big] \\
&= \mathbb{P}\Big[h_s > \frac{\gamma(I+\sigma^2)}{p\, g_{max}\, K\, S_{th}} \Big| S_{th}, \phi_0^r\Big] \\
&\overset{(a)}{=} \sum_{k=0}^{m_s-1} \frac{(-s)^k}{k!}\left[\frac{\partial^k \mathcal{L}_{I_{tot}}(s|S_{th}, \phi_0^r)}{\partial s^k}\right]_s \\
&\overset{(b)}{=} \sum_{i=1}^{2^m}\sum_{k=0}^{m_s-1}\int_{w_{min}}^{\infty} \frac{(-s)^k}{k!}\left[\frac{\partial^k \mathcal{L}_{I_{tot}}(s|S_{th}, \phi_0^i)}{\partial s^k}\right]_s \\
&\quad \times f_S(S_{th}) p_\phi \mathrm{d}S_{th},
\end{aligned} \quad (14)$$

where (a) follows from the complementary cumulative distribution function (cdf) of h_s, the definition of incomplete gamma function for integer values of m_s and by using $\mathbb{E}_{I_{tot}}[\exp(-sI_{tot})(sI_{tot})^k] = (-s)^k \frac{\partial^k \mathcal{L}_{I_{tot}}(s)}{\partial s^k}$, and (b) follows from deconditioning over the maximum power S and all possible receiving beam's maxima ϕ_0^r with the pdf $f_S(s_0)$ and the pmf p_ϕ, respectively. ■

Remark 1. *The coverage probability is a sum of 2^m conditional coverage probability terms, conditioned on all possible receiving beams. Moreover, the conditional coverage probability is first obtained conditioned on the maximum received power. This is a consequence of both the Euclidean and the angular distances which are considered while determining the serving BS through exhaustive scanning.*

Having derived the coverage probability, the rate coverage can be obtained as

$$\begin{aligned}
\mathcal{R}_c(R_{th}) &= \mathbb{P}[B_w \log_2(1+\mathrm{SINR}) \ge R_{th}]) \\
&= \mathcal{P}_c(2^{R_{th}/B_w} - 1),
\end{aligned} \quad (15)$$

and the average achievable rate of the UE can be obtained as

$$\begin{aligned}
\mathcal{R} &= \mathbb{E}[B_w \log_2(1+\mathrm{SINR})]) \\
&= \frac{B_w}{\ln 2}\int_0^\infty \frac{\mathcal{P}_c(\gamma_{th})}{1+\gamma_{th}}\mathrm{d}\gamma_{th} \\
&\overset{(a)}{=} \frac{B_w}{\ln 2}\int_0^\infty \mathcal{P}_c(e^t - 1)\mathrm{d}t,
\end{aligned} \quad (16)$$

where (a) follows through the change of variable $\gamma_{th} + 1 = e^t$.

IV. Results and Discussions

In this section, numerical results are presented to evaluate and compare the performance achieved in a dense mmWave cellular network. The accuracy of the analytical results is verified by comparing them with the empirical results obtained from Monte-Carlo simulations. For all numerical results, the following parameters have been used unless stated otherwise: $R_L = 75$ meters, $\alpha_L = 2$, $f_c = 26.5$ GHz as in [5]. As per the 3GPP specifications $p = 45$ dBm, $\sigma^2 = -74$ dBm, $\lambda_{bs} = 0.0008$ BSs/m^2 and $m_u = 2$. The receiver is assumed to be equipped with a directional antenna with 4 sectors, i.e., $m = 2$ and $\phi_{3dB} = \pi/2$. In order to focus on spectral efficiency, we will normalize the achievable rate by B_w, which is equivalent to considering $B_w = 1$ in (15) and (16).

Fig. 2 presents the coverage probability versus γ_{th} for different numbers of beams/sectors produced by the receiver antenna and for two values of α_L. For completeness, the coverage probability of an ideal baseline scenario where the directions of the maximum gains at the serving BS and receiver are fully aligned, is also depicted. It is observed that the coverage performance of the network under the ideal baseline scenario is clearly overestimated. Note that, under the 5G NR

$$\mathcal{L}_I(s|S_{th}, \phi_0^r) = \exp\Big(-\lambda_{bs}\int_{\mathbf{\Omega}}\Big(1 - \Big(1 + \frac{s\, p\, K\, g_{max}\, g_{3gpp}(|\phi_0^r - \phi_x|)\, r_x^{-\alpha_L}}{m_x}\Big)^{-m_x}\Big) r_x \mathrm{d}\mathbf{\Omega}\Big), \quad (11)$$

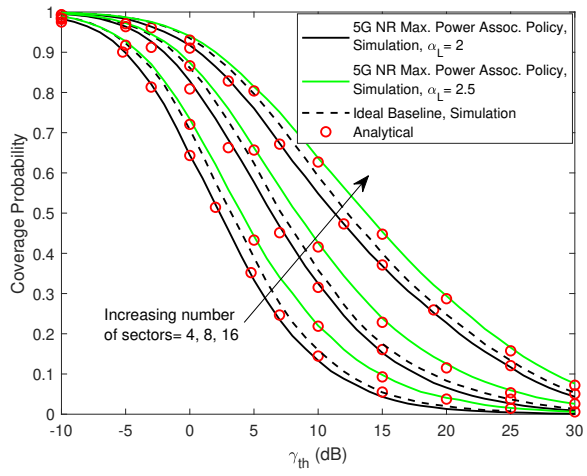

Fig. 2: Coverage probability versus γ_{th} for different number of beams/sectors and for two values of α_L. An ideal baseline scenario, with perfect beam alignment is also depicted.

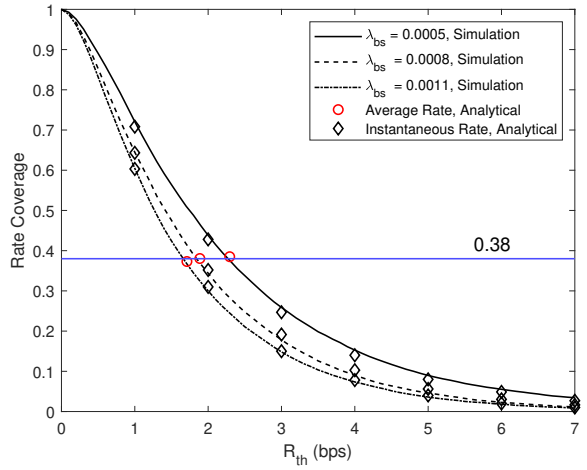

Fig. 3: The rate coverage versus R_{th} for different values of λ_{bs}. The red and black markers denote the analytical average and instantaneous rate, respectively.

maximum power association policy, the receiver performs exhaustive scanning in each sector to select the BS that provides the maximum power. The number of beams/sectors of the receiver's antenna affects both the desired received power and the interference power falling within the 3dB beamwidth of the receiver's antenna pattern. Indeed, as the number of sectors increases, the receiver minimizes the misalignment error. At the same time, the receiver's beams become highly-directional, thus decreasing the aggregate interference power. Finally, it can be observed that the coverage probability degrades with a decrease in the path-loss exponent. While reducing α_L increases the received signal power, it also increases the aggregate interference power due to the favorable path loss conditions, thus degrading the coverage performance.

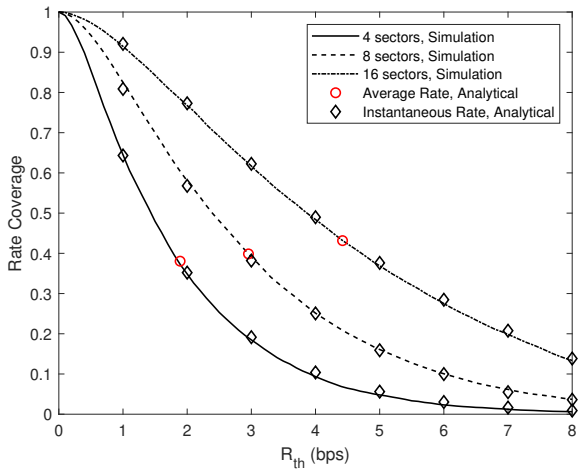

Fig. 4: The rate coverage versus R_{th} for different number of beams/sectors. The red and black markers denote the analytical average and instantaneous rate, respectively.

Fig. 3 presents both the empirical, via simulation, and the analytical, evaluated through (15), rate coverage versus R_{th} for different values of λ_{bs}. The average achievable rate, which is evaluated analytically using (16), for each curve is also illustrated. Accordingly, the probability that the instantaneous link rate is above the average achievable rate is also demonstrated. The first observation is that with the increase of the BSs' deployment density, the probability that the instantaneous achievable rate is above a target rate, decreases. However, the degradation in the performance of the achievable rate becomes less severe with the increase of λ_{bs}. Moreover, it is observed that the probability of achieving the average rate is approximately 38% for all values of λ_{bs}.

Fig. 4 presents both the empirical, via simulation, and the analytical, evaluated through (15), rate coverage versus R_{th} for different number of sectors/beams. The average achievable rate, which is evaluated analytically using (16), for each curve is also illustrated. Accordingly, the probability that the instantaneous link rate is above the average achievable rate is also demonstrated. As expected, the probability of achieving a target value increases with the increase in the number of sectors/beams. An interesting observation is that the right most curves preserve larger achievable rate but at the expense of a significantly increased variance. Moreover, as the UE's beams become more directional, the probability of achieving the average value is increasing.

V. Conclusions

In this work, a novel stochastic geometry framework was proposed for mmWave cellular networks to address the role of the angular distances in a maximum power based association policy under a realistic beam management procedure. To this end, both the Euclidean and the angular distances were considered in the analysis of cell association, which is a key novelty of this paper. Moreover, the impact of angular distances in the

misalignment error was captured. As key system-level insights, it was shown that: i) as the BSs' deployment density increases, the performance in terms of the instantaneous achievable rate degrades. However, the rate of degradation gets smaller with the increase of BS densities, and ii) As the UE's beams become more directional, the instantaneous achievable rate gets larger but at the expense of a significantly higher variance. Furthermore, the probability of achieving the higher rate than the average increases with the BS density.

APPENDIX A
PROOF OF LEMMA 2

The pdf of S_x is first derived. Since $\varphi_r \sim U[0, \frac{\phi_{3dB}}{2}]$, $g(\varphi_r) = 10^{\frac{G_{max}-12\left(\frac{\varphi_r}{\phi_{3dB}}\right)^2}{10}}$. Clearly, $g(\varphi_r)$ is a function of the random variable φ_r. Building on φ_r and applying successive change of variables, the pdf $f_{g(\varphi_r)}(g)$ is given by

$$f_{g(\varphi_r)}(g) = \frac{1}{ln(10)x}\frac{10}{12\sqrt{\frac{G_{max}-10log(x)}{12}}}, \quad x \in [g_{3dB}, g_{max}]. \tag{17}$$

Subsequently, the pdf of $r_x^{-\alpha_L}$ is expressed in terms of the corresponding cdf as

$$\begin{aligned}\mathbb{P}[r_x^{-\alpha_L} \leq x] &= \mathbb{P}\Big[r_x^{\alpha_L} \geq \frac{1}{x}\Big] = 1 - \mathbb{P}\Big[r_x \leq \Big(\frac{1}{x}\Big)^{\frac{1}{\alpha_L}}\Big] \\ &= 1 - F_{r_x}\Big(\Big(\frac{1}{x}\Big)^{\frac{1}{\alpha_L}}\Big), \quad F_{r_x}(r) = \frac{r^2}{R_L^2}.\end{aligned} \tag{18}$$

Now, $f_{r_x^{-\alpha_L}}(x)$ is obtained after differentiating (18) w.r.t the appropriate range of x, that is,

$$f_{r_x^{-\alpha_L}}(x) = \frac{2\left(\frac{1}{x}\right)^{\frac{\alpha_L+2}{\alpha_L}}}{\alpha_L R_L^2}, \quad x \in [R_L^{-\alpha_L}, \infty). \tag{19}$$

The pdf and the cdf of S_x can now be written as

$$f_{S_x}(w) = \int_{g_{3dB}}^{\psi(w)} \frac{1}{x} f_{g(\varphi_r)}(x) f_{r_x^{-\alpha_L}}\Big(\frac{w}{x}\Big)\mathrm{d}x, \tag{20}$$

$$F_{S_x}(w_0) = \int_{g_{3dB}R_L^{-\alpha_L}}^{w_0}\int_{g_{3dB}}^{\psi(w)} \frac{1}{x} f_{g(\varphi_r)}(x) f_{r_x^{-\alpha_L}}\Big(\frac{w}{x}\Big)\mathrm{d}x\mathrm{d}w. \tag{21}$$

The pdf of $S = \max_{x\in\Psi_{bs}}\{S_x\}$ can now be obtained by exploiting the theory of Order Statistics [19]. Let T_k define the event $T_k = \{\text{k BSs exist in } \mathbf{b}(\mathbf{o}, R_L)\}$. Then, from the definition of Ψ_{bs}, $\mathbb{P}[T_k] = e^{-\lambda_{bs}\pi R_L^2}(\lambda_{bs}\pi R_L^2)^k/k!$. Given T_k and since the elements of S_x are i.i.d., the probability that $S \leq s_0$ is given by $\mathbb{P}[S \leq s_0|T_k] = F_S(s_0|T_k) = (F_{S_x}(w))^k$. Now, $F_S(s_0)$ can be obtained by deconditioning over T_k, that is

$$\begin{aligned}F_S(s_0) &= F_S(s_0|T_k)\mathbb{P}[T_k] \\ &\overset{(a)}{=} \sum_{k=0}^{\infty}(F_{S_x}(w))^k e^{-\lambda_{bs}\pi R_L^2}\frac{(\lambda_{bs}\pi R_L^2)^k}{k!} \\ &\overset{(b)}{=} e^{-\lambda_{bs}\pi R_L^2\left(1-F_{S_x}(s_0)\right)}, \quad s_0 \in [w_{min}, \infty),\end{aligned} \tag{22}$$

where (a) follows after averaging over k and (b) follows from $\sum_{k=0}^{\infty}\frac{a^k b^k}{k!} \overset{\triangle}{=} e^{ab}$. Finally, the pdf $f_S(s_0)$ is obtained as $f_S(s_0) = \frac{dF_S(s_0)}{ds_0} = \lambda_{bs}\pi R_L^2\, f_{Pr_x}(s_0)\, e^{\lambda_{bs}\pi R_L^2\left(F_{S_x}(s_0)-1\right)}$.

ACKNOWLEDGMENT

This work has been partly supported by the University of Piraeus Research Center (UPRC). H. S. Dhillon gratefully acknowledges the support of US NSF (Grants CNS-1923807 and CNS-2107276).

REFERENCES

[1] S. Tripathi, N. V. Sabu, A. K. Gupta, H. S. Dhillon, "Millimeter-wave and Terahertz Spectrum for 6G Wireless", in 6G Mobile Wireless Networks. Y. Wu, S. Singh, T. Taleb, A. Roy, H. S. Dhillon, M. R. Kanagarathinam, A. De, eds. Springer, pp. 83-121, 2021.

[2] M. Xiao et al., "Millimeter wave communications for future mobile networks," *IEEE J. Sel. Areas Commun.*, vol. 35, no. 9, pp. 1909–1935, Sep. 2017.

[3] S. He et al., "A survey of millimeter-wave communication: Physical layer technology specifications and enabling transmission technologies," *Proc. IEEE*, vol. 109, no. 10, pp. 1666–1705, Oct. 2021.

[4] H. Wei, N. Deng and M. Haenggi, "Performance Analysis of Inter-Cell Interference Coordination in mm-Wave Cellular Networks," *IEEE Trans. Wireless Commun.*, vol. 21, no. 2, pp. 726-738, Feb. 2022.

[5] S. S. Kalamkar, F. Baccelli, F. M. Abinader, A. S. M. Fani and L. G. U. Garcia, "Beam Management in 5G: A Stochastic Geometry Analysis," *IEEE Trans. Wireless Commun.*, vol. 21, no. 4, pp. 2275-2290, Apr. 2022.

[6] N. Kouzayha, H. Elsawy, H. Dahrouj, K. Alshaikh, T. Y. Al-Naffouri and M. -S. Alouini, "Analysis of Large Scale Aerial Terrestrial Networks with mmWave Backhauling," *IEEE Trans. Wireless Commun.*, vol. 20, no. 12, pp. 8362-8380, Dec. 2021.

[7] X. Yu, J. Zhang, M. Haenggi, and K. B. Letaief, "Coverage analysis for millimeter wave networks: The impact of directional antenna arrays," *IEEE J. Sel. Areas Commun.*, vol. 35, no. 7, pp. 1498–1512, Jul. 2017.

[8] N. Deng and M. Haenggi, "A Novel Approximate Antenna Pattern for Directional Antenna Arrays," *IEEE Wireless Commun. Lett.* , vol. 7, no. 5, pp. 832-835, Oct. 2018.

[9] M. Giordani et al., "A tutorial on beam management for 3GPP NR at mmWave frequencies," *IEEE Commun. Surveys Tuts.*, vol. 21, no. 1, pp. 173–196, 1st Quart., 2018.

[10] A. G. Kanatas, "Coordinates Distributions in Finite Uniformly Random Networks," *IEEE Access*, vol. 10, pp. 49005-49014, 2022.

[11] C. K. Armeniakos and A. G. Kanatas, "Angular Distance-Based Performance Analysis of mmWave Cellular Networks," *IEEE Global Commun. Conf. (GLOBECOM)*, pp. 5432-5437, Dec. 2022.

[12] M. Rebato, L. Resteghini, C. Mazzucco and M. Zorzi, "Study of Realistic Antenna Patterns in 5G mmWave Cellular Scenarios," *IEEE Int. Conf. Commun.*, pp. 1-6. 2018.

[13] J. Wildman, P. H. J. Nardelli, M. Latva-aho and S. Weber, "On the Joint Impact of Beamwidth and Orientation Error on Throughput in Directional Wireless Poisson Networks," *IEEE Trans. Wireless Commun.*, vol. 13, no. 12, pp. 7072-7085, Dec. 2014.

[14] A. Thornburg, T. Bai and R. W. Heath, "Performance Analysis of Outdoor mmWave Ad Hoc Networks," *IEEE Trans. Signal Process.*, vol. 64, no. 15, pp. 4065-4079, Aug. 2016.

[15] J. G. Andrews, T. Bai, M. N. Kulkarni, A. Alkhateeb, A. K. Gupta, and R. W. Heath, "Modeling and analyzing millimeter wave cellular systems," *IEEE Trans. Commun.*, vol. 65, no. 1, pp. 403–430, Jan. 2017.

[16] K. Humadi, I. Trigui, W. -P. Zhu and W. Ajib, "User-Centric Cluster Design and Analysis for Hybrid Sub-6GHz-mmWave-THz Dense Networks," *IEEE Trans. Veh. Technol.*, vol. 71, no. 7, pp. 7585-7598, Jul. 2022.

[17] T. Bai and R. W. Heath, "Coverage and rate analysis for millimeterwave cellular networks," *IEEE Trans. Wireless Commun.*, vol. 14, no. 2, pp. 1100–1114, Feb. 2015.

[18] C. K. Armeniakos, A. G. Kanatas, and H. S. Dhillon, "Comprehensive Analysis of Maximum Power Association Policy for Cellular Networks Using Distance and Angular Coordinates," Mar. 2023, arXiv:2303.09939.

[19] M. Ahsanullah, V. Nevzorov and M. Shakil, *An Introduction to Order Statistics*. Atlantis Press, 2013.